EARLY, NON-CILIARY ROLE FOR MICROTUBULE PROTEINS IN LEFT-RIGHT PATTERNING IS CONSERVED ACROSS KINGDOMS

Maria Lobikin[1], Gang Wang[2], Jing-Song Xu[2], Yi-Wen Hsieh[3], Chiou-Fen Chuang[3],

Joan M. Lemire[1], and Michael Levin[1]*

(1) Center for Regenerative and Developmental Biology, and
Department of Biology
Tufts University
200 Boston Ave.
Medford, MA 02155 U.S.A.

(2) University of Illinois College of Medicine
Chicago, IL

(3) Division of Developmental Biology
Cincinnati Children's Hospital Research Foundation
Cincinnati, OH

* Author for Correspondence
Tel. (617) 627-6161
Fax: (617) 627-5035
email: michael.levin@tufts.edu

Classification: BIOLOGICAL SCIENCES: Developmental Biology
Running title: Conserved tubulin role in asymmetry
Keywords: tubulin, Xenopus, C. elegans, left-right asymmetry, laterality

ABSTRACT

Many types of embryos' bodyplans exhibit consistently-oriented laterality of the heart, viscera, and brain. Errors of left-right patterning present an important class of human birth defects, and considerable controversy exists about the nature and evolutionary conservation of the molecular mechanisms that allow embryos to reliably orient the left-right axis. Here we show that the same mutations in the cytoskeletal protein tubulin that alter asymmetry in plants also affect very early steps of left-right patterning in nematode and frog embryos, as well as chirality of human cells in culture. In the frog embryo, tubulin α and tubulin γ-associated protein are required for the differential distribution of maternal proteins to the left or right blastomere at the first cell division. Our data reveal a remarkable molecular conservation of mechanisms initiating left-right asymmetry. The origin of laterality is cytoplasmic, ancient, and highly conserved across kingdoms – a fundamental feature of the cytoskeleton that underlies chirality in cells and multicellular organisms.

/body

INTRODUCTION

Consistent laterality is a fascinating aspect of embryonic development and has considerable implications for the physiology and behavior of the organism. Although vertebrates are generally bilaterally symmetric externally, most internal organs, such as the heart, viscera, and brain display asymmetric structure and/or unilateral positioning with respect to the left-right (LR) axis. A common defect in left-right (LR) patterning is the loss of concordance among the sidedness of individual organs known as heterotaxia. In human beings, abnormalities in the proper development of laterality occur in more than 1 in 8000 live births and often have significant medical consequences (1). Organ asymmetry is highly conserved among species; however considerable controversy exists about the early steps of LR patterning among phyla (2-4).

One model predicts that cilia-driven extracellular fluid flow during gastrulation is the origin of LR asymmetry (5). Because numerous species initiate asymmetry prior to (or without) the presence of cilia (6, 7), and because "ciliary" proteins, such as *left-right dynein*, known to be important for LR patterning also have intracellular roles compatible with cilia-independent functions in laterality (8-11), it is widely thought that asymmetry generation is poorly conserved, with numerous distinct mechanisms used throughout phyla. In contrast, we have suggested that asymmetry may be an ancient, well-conserved property of individual cells arising from the chirality of cytoskeletal structures that is subsequently amplified by physiological mechanisms (4, 11, 12). Thus, we sought the most evolutionarily-distant model systems, and ones that are known not to rely on cilia for left-right patterning, to test the hypothesis of fundamental molecular conservation of asymmetry mechanisms.

Recent findings in *Arabidopsis thaliana* have shown that mutations in α-tubulin and in a γ-tubulin-associated protein (Tubgcp2) play an important role in the symmetry properties of the plant's

axial organs (13-15). Wild-type *Arabidopsis thaliana* axial organs do not twist during normal elongation, and its flowers are radially symmetrical. This symmetry can be broken by mutations in tubulin and tubulin-associated protein complexes. The tubulin mutations *spiral1, spiral2, spiral 3* produce right-handed helical growth mutants. *Lefty (lefty1* and *lefty2)* mutants were found to be suppressor mutants of *spiral1*, and when outcrossed displayed a prominent left-handed helical growth (13, 15). Both α-tubulin and γ-tubulin complexes are ubiquitous in eukaryotes and are involved in the formation and nucleation of microtubules. Here, we characterize the laterality phenotypes induced by the same mutations in a vertebrate embryo (the frog *Xenopus laevis*), the nematode *C. elegans*, and mammalian cells in culture, supporting a fundamental role for tubulin in the cilia-independent generation of left-right asymmetry.

RESULTS

To determine whether the same tubulin proteins implicated in *Arabidopsis* asymmetry also play a role in the large-scale asymmetry of both vertebrate and plant systems, homologous mutations were made in *Xenopus laevis* α tubulin and γ tubulin-associated protein Tubgcp2 (Fig. S1). These mutations have already been shown in microtubule ultrastructure studies to function as dominant negatives when assembled into the cytoskeleton together with native subunits (16, 17). Synthetic mRNAs encoding these mutant tubulins were then injected into *Xenopus* embryo blastomeres (at various early stages) using standard methods (18); Western blot analysis indicated that when injected at the 1-cell stage, the amount of exogenous mutant protein at 4-cell stage was similar to that of the native wild-type tubulin in the cell (quantification of Western blot showed a 170% increase in α-tubulin and a 190% increase in Tubgcp2 at 4-cell stage following 1-cell injections). At st. 45, embryos were analyzed for position (situs) of the heart, stomach and gallbladder (Fig 1a-c) – a definitive readout of LR patterning. All treatments were titered to avoid non-specific defects (resulting in embryos with perfectly normal dorsoanterior development, clear left- or right-sided organs with normal morphology, correct size and relative proportions, and wild-type behavior), thus ruling out general toxicity as a cause of LR phenotypes.

Embryos injected immediately after fertilization with mRNA encoding the dominant negative mutant α-tubulin (tub4a) displayed significant levels of heterotaxia (independently randomized sidedness of the 3 scored organs, Fig 1d), revealing a common genetic underpinning of regulation of asymmetry between plant and vertebrate systems. Injections of wild-type tub4a mRNA had no effect on asymmetry. Co-injections of both mutants' mRNAs together did not significantly increase the incidence of heterotaxia, suggesting that these impact the same pathway (are not additive). We next introduced the mutant mRNAs at different timepoints during development, to determine when the tubulins

functioned in left-right patterning and to test the possibility that the relevant tubulin structures are those in the cilia at the ciliated organ (GRP).

Synthetic mRNAs injected immediately after fertilization are already translated by the 2-cell stage (Fig S2 and protein level quantification above); studies of GRP and cilia routinely inject at the 4-cell stage to target functional reagents to this structure (19). If tubulins were to function in LR asymmetry at any time *after* the first few cleavages (e.g., in the GRP during neurulation), injections at the 2- or 4-cell stages would show the same randomizing effects on asymmetry as do injections at the 1-cell stage. In contrast, injections of mutant tub4a mRNA into both blastomeres of the 2-cell embryo (or later) had no effect on asymmetry. The mutant tubulin's introduction into very early embryos randomizes LR patterning when present during the earliest events of cleavage-stage development, but cannot affect the LR axis when introduced as early as the 2-cell stage, ruling out involvement in LR patterning steps occurring after the first cleavages. Injections were also made in 4-cell stage embryos, in either the left-dorsal (LD) blastomere, which is known to be an early precursor of the ciliated organ and crucial for nodal flow (19) or the right-ventral (RV) cell, whose descendants do not contribute to the frog node (20) (GRP). Neither injection made at the 4-cell stage produced significant levels of heterotaxia (Fig 1d), a result incompatible with mutant α-tubulin affecting asymmetry via impact upon cilia-related events at the node. The same results were obtained using injections of mRNA encoding mutated γ-tubulin associated protein (tubgcp2) mRNA (Fig. 1f,g). Our data reveal that the same functions of tubulin that alter asymmetry in a plant species are also involved in LR patterning in frog embryos, and that this function takes place very early (at the first cleavage).

To determine whether the tubulin-regulated events function in the same pathway as known early LR mechanisms and likewise control downstream asymmetric transcription, we investigated whether the expression of tubulin mutants perturbed the normally left-sided expression of the earliest

known asymmetric gene in *Xenopus*: the TGF-β signaling factor Nodal (Xnr-1) (21). Xnr-1 is normally expressed only on the left side of the embryo at approximately stage 22(22). Embryos injected with mutated tubulin mRNAs at the one-cell stage were fixed at stage 22 and processed for *in situ* hybridization with an *Xnr-1* probe. A significant percentage (64.7% for tub4a and 32.5% for tubgcp2) of mutant-injected embryos displayed randomized *Xnr-1* expression (Fig 2), suggesting that these tubulin mutations affect LR asymmetry upstream of *Nodal* expression.

One model explaining the effect of the tubulin mutations on asymmetry is that they perturb the normal rightward bias that has been found in the intracellular transport vector provided by the cytoskeleton in cleavage-stage frog embryos (23, 24). These oriented cytoskeletal tracks allow cytoplasmic motors, such as kinesins and dyneins, to localize specific protein cargo to the L or R sides; while we previously characterized several specific maternal proteins that exhibited such cytoskeleton-dependent asymmetric localization (25-27), we now sought a comprehensive analysis of asymmetric maternal components in the early embryo, and wanted to determine which of these were dependent on tubulin (thus identifying also those asymmetric *Xenopus* proteins for which no immunohistochemistry-suitable antibody is available). We performed a quantitative proteomics profiling of the left and right sides of 4-cell embryos. Control embryos, and those injected at the 1 cell stage with either the tub4a or tubgcp2 mutant, were fixed in methanol at the 4-cell stage, oriented, and split along the left-right axis (1^{st} cleavage plane) with a blade. The L and R sides were pooled (N=50), and samples were analyzed via liquid chromatography-mass spectrometry. Proteins showing a significant ($p<0.05$, ANOVA) (more than 3-fold difference in either direction) left- or right-sided bias in control embryos were selected. The analysis confirmed asymmetric localization of ion transporters (Tables S2A-S2B) and the higher frequency of right-biased targets, which has been noted in previous work (24, 26, 27). In a number of instances, the presence of mutated tubulin significantly affected the endogenous bias in localization,

either reversing or completely abolishing it (Tables S2A-S2B). As expected, this included cytoskeletal and transport-related proteins such as dynactin, cofilin-1, and a nonmuscle myosin (Table 1).

Cofilin-1, an actin depolymerization and filament severing protein(28), was chosen for further investigation because of the known importance of actin in early cytoskeletal organization, Cofilin's role in directing the intracellular trafficking of ion transporter cargo (29), and recent data showing cofilin is asymmetrically transcribed in the 2-cell murine embryo (30). Injections into fertilized eggs of either tdTomato:Cofilin-1a alone, or in conjunction with a tubulin mutant, were analyzed for tdTomato localization (Fig 3a-b, d) at st. 45, where the embryo's transparency allowed clear detection of which side's progenitor cells had inherited the tagged cofilin (Figure S4). While injections of tdTomato alone showed no significant bias in localization, tdTomato:Cofilin-1a injections revealed a significant ($p<<0.01$, paired t-test) leftward bias in the fluorescent signal (Left localized : Right localized ratio of 1.35), confirming that cofilin protein is indeed localized asymmetrically during the first cleavages. Co-injections of either of the tubulin mutants together with the tdTomato:cofilin-1a significantly ($p<0.05$) altered the normal left-ward bias of cofilin localization, and lead to subsequent randomization of organ situs (Fig. S3). Co-injection with the tuba4 mutant resulted in a 0.91 L:R bias, thus abolishing cofilin's leftward bias, while the tubgcp2 mutant resulted in a 0.69 L:R ratio, reversing the bias (Fig 3c). Scoring organ situs in tdTomato:cofilin-injected embryos revealed a weak but significant (8%) incidence of heterotaxia, consistent with some impairment of the interaction of cofilin with the LR localization machinery due to the addition of a large tdTomato structure (thus likely artificially lowering the bias in localization we observed). Taken together, these results suggest that the tubulin mutations are perturbing the normal consistent left-right bias of a range of maternal proteins at the 4-cell stage, consistent with models in which cytoskeletal organization drives positioning of LR-relevant cargo during the first cleavages in the *Xenopus* embryo.

Having observed the remarkable conservation of asymmetry roles for tubulin proteins between frog and *Arabidopsis*, we tested the same mutations in two additional model systems: the nematode *C. elegans*, and human HL60 cells, thereby covering an extremely broad range of asymmetry types and bodyplans.

The two "AWC" olfactory neurons of *C. elegans* are morphologically symmetric, but display asymmetric expression of chemosensory receptors along the left-right axis. Wild-type animals generate one AWC^{ON} cell, which expresses the reporter gene *str-2p::GFP*, and one AWC^{OFF} cell, which does not (Fig. 4A-C) (31). Specific disruption of microtubules in AWC by nocodazole and benomyl generates 2 AWC^{ON} neurons, suggesting that microtubules are required for left-right AWC neuronal asymmetry (32). *C. elegans* TBA-9 α-tubulin shares 75% identical amino acids with *A. thaliana* TUA6 α-tubulin. We mutated the conserved aspartic acid (256th) and glutamic acid (259th) residues in TBA-9 to alanine and expressed the TBA-$9^{D256A/E259A}$ mutant protein in AWC under the control of the *odr-3* promoter. Like nocodazole treatment, expression of TBA-$9^{D256A/E259A}$ caused a 2 AWC^{ON} phenotype at a frequency significantly higher than that caused by expression of wild-type TBA-9 when injected at the same concentration (Fig. 4C). Both *odr-3p::tba-9* and *odr-3p::tba-*$9^{D256A/E259A}$ transgenes also caused a weak 2 AWC^{OFF} phenotype. These results suggest that the two conserved residues in the GTPase-activating domain of α-tubulins regulate microtubule dynamics required for precise left-right patterning of *C. elegans*.

An important recent finding is the observation that mammalian cells in culture, having neither node-like structure, nor cilia-derived fluid flow, establish and maintain consistent left-right asymmetries with respect to axes defined by internal polarity markers (33, 34). Neutrophil-like HL-60 cells in culture extend pseudopodia to the left of an axis drawn between the nucleus and centrosome (34). To test whether this asymmetry likewise depended on functional tubulin proteins, we transfected differentiated

HL-60 cells with GFP-Arrestin-3 (a marker of the microtubule organizing center) and one of the mutant constructs: wild type tub-a6 (Fig. 4D), or mutant tub-a6 (Fig. 4E). While wild-type tub-a6 (at expression levels achievable by transfection) did not affect the leftward bias, mutant tub-a6 abolished it. Thus, the same tubulin mutations that specifically randomize asymmetry in plant, vertebrate and nematode systems likewise do so in a mammalian system.

DISCUSSION

The ciliary flow paradigm must postulate highly divergent origins of asymmetry (all feeding into the same Nodal-Pitx cascade), because numerous invertebrate phyla establish consistent LR asymmetry without cilia or a node. Moreover, neither the pig nor the chick utilize cilia in their LR patterning pathway (7, 35); zebrafish (36-38) and mouse (39) mutants now exist that exhibit normal asymmetry despite ciliary defects, and even mouse embryos already have LR non-equivalent blastomeres by the third cleavage (40). Thus we sought to test a model of much earlier asymmetry-determining processes that would exhibit a more satisfying evolutionary conservation across a wide range of phyla.

Our data show that the presence of well-characterized mutant forms of either α- or γ- tubulin subunits in frog embryos specifically randomizes the LR axis (Fig. 1), controlling the LR pathway upstream of the well-conserved asymmetric expression of *Nodal* (Fig. 2). While the levels of heterotaxia were clearly significantly different from controls, they were below the ~87% theoretical maximum (for 3 fully-randomized organs) because of the need to titer the mRNA to low levels. Despite the crucial housekeeping roles of tubulin, we were able to find a level of expression of mutants that allowed dissection of their LR patterning roles independent of any toxicity or generalized teratology.

Varying the timing of injection allowed us to place strict bounds on the timing of the activity of these proteins in the LR pathway. It is clear that protein has already been made from microinjected mRNA by ~30 minutes after fertilization (Fig. S2). Strikingly, while 1-cell injections randomized asymmetry, injections at the 2- or 4-cell stage were already too late to do so (Fig. 1D), suggesting that the function of tubulin in asymmetry occur no later than approximately the 4- or 8-cell stage (because 2-cell injections produce protein by then). Most crucially, injections of both cells at the 2-cell stage do not affect asymmetry, ruling out interference with cilia-driven events at the GRP as the mechanism by which these mutants randomize the LR axis. While the GRP can be affected by reagents injected at 4-cell stage

(19), we show that expressing mutant tubulin in GRP cells makes no difference to asymmetry; the factor that determines whether or not the LR axis will be randomized is whether the mRNA was injected prior to the 2-cell stage and thus was available for translation during the earliest stages of development. Thus, the need to function during the first few cleavages of the embryo (Fig. 1) is incompatible with explanations involving the GRP's cilia or nodal flow. The data are however consistent with models in which the early cytoskeleton is nucleated by a chiral structure (41) that orients itself with respect to the other two axes, and thus biases the intracellular transport of key determinants along the LR axis (11, 42). One such model is shown in Fig. S5, although elaborating the precise details will require development of smaller fluorescent tags, since fusion of GFP to the mutant tubulin (in attempts to visualize their subcellular localization) resulted in high levels of toxicity and LR randomization.

As has been shown in snail embryos (43), early cytoskeletal dynamics are transduced into changes of asymmetric gene expression. How does this occur in *Xenopus*? We have previously shown that the integrity of the cytoskeleton at the first few cleavages is crucial for the correct asymmetric localization of several maternal proteins whose activity is in turn transduced into asymmetric transcription (24, 27, 44), and that by the 2nd cell cleavage the cytoskeleton already exhibits a directionality leading kinesin-associated cargo (or marker molecules) to the right side (24). Others have shown that a pre-existing consistent chirality of the cytoskeleton exists in the egg cortex (45). In order to get the first unbiased glimpse of asymmetries existing very soon after establishment of the midline, we performed a proteomic analysis. This revealed a number of proteins with significant LR bias at the 4-cell stage (Tables S2A,S2B). While the functions of these asymmetrically-localized proteins remain to be probed by future studies, these data confirm the existence of consistent molecular asymmetries at very early stages (long before gastrulation) (25, 27, 45, 46), and exhibit a relative enrichment of right-sided proteins as found in our previous drug screens (which so far have identified only right-sided targets).

While the large yolky cells of the early frog embryos are not conducive to the high-resolution imaging of cytoskeletal structure needed to identify subtle changes in chirality, the proteomic data reveal the consequences of tubulin mutation for the asymmetric distribution of early embryonic components, despite the unavailability of antibodies for most of these frog proteins. Analysis of protein distribution after microinjection of the two mutant tubulin mRNAs revealed (Table 1) that a number of important signaling proteins become mislocalized. Thus, we propose that the role of tubulins during early development is to serve as components of the chiral cytoskeleton by means of which asymmetric components sort to the L and R sides during the first cleavages, and as an important component of other intracellular localization events taking place at the 2-8 cell stages. We selected one protein – cofilin, and labeled it with a fused fluorescent protein. While this also had somewhat of a destabilizing effect on asymmetry (Fig. S3, suggesting a functional role for cofilin), nevertheless we were able to observe a statistically significant bias in its native localization (Fig. 3C,D) and showed that this native LR bias is abolished when tubulin mutants are introduced in the 1-cell embryo.

Our data support previous models in which cytoskeletal chirality is amplified via differences in intracellular transport of key cargo during very early stages (23, 42, 47, 48). Although the details are somewhat different, that same scheme is utilized by snail (43) and C. elegans (32) embryos. Perhaps the most remarkable aspect of these data is the wide-spread evolutionary conservation (even across the independent origin of multicellularity in plants and animals) of the role of these tubulin proteins in asymmetry, extending to plant coiling (14), *C. elegans* asymmetric neural patterning (Table 2), pseudopodial asymmetries in human cells in culture (Fig. 4), and organ placement of the vertebrate *Xenopus* laevis (Fig. 1). This is consistent with the non-ciliary roles for tubulin in frog asymmetry, as neither nematodes nor plants nor HL60 cells utilize cilia in their asymmetry pathways. We have previously stressed the evolutionary conservation of several asymmetry-amplifying mechanisms across multiple diverse taxa (6, 11, 12, 49). The above results are the first data that implicate a single protein as

an ancient, fundamental element with a highly conserved role as the initiator chirality, upon which very different bodyplans can establish consistent downstream asymmetries of form and function.

MATERIALS and METHODS

Constructs

Frog: Plasmids containing *X.laevis* tuba4 and Tubgcp2 (Xgrip110) and cofilin cDNA were purchased from Open Biosystems (Clone IDs: 7010865,5078639, and 5571290 respectively). The coding regions of these cDNAs were amplified by PCR inserted pCS2+ expression vectors using the In-Fusion® Advantage PCR Cloning kit (Clontech). Tuba4 pCS2 and TubGCP2 pCS2 plasmids were linearlized with Acc65I to prepare for transcription with the SP6 Message machine kit (Ambion). Tuba4-mut (Ala180 replaced with Phe) and tubgcp2-mut (Gly453 replaced with Arg) were generated using the Quikchange II Site-directed Mutagenesis Kit (Stratagene). Nematode: Full-length *tba-9* cDNA (1368 bp) was obtained with RT-PCR of total mRNA from mixed stage worms and were subcloned to make *odr-3p::tba-9::SL2::TagRFP*. *odr-3p::tba-9*$^{D256A/E259A}$*::SL2::TagRFP* was generated by site-directed mutagenesis (Stratagene QuikChange kit). *odr-3p::tba-9::SL2::TagRFP* (50 ng/µl) and *odr-3p::tba-9*$^{D256A/E259A}$*::SL2::TagRFP* (50 ng/µl) were injected into animals as described (50). The coinjection marker *ofm-1p::DsRed,* which is expressed in the coelomocytes, was injected at 30 ng/µl.

Animal Husbandry

Xenopus embryos were collected and maintained according to standard protocols (18) in 0.1X Modified Marc's Ringers (MMR), pH 7.8 with 0.1% Gentamicin, and staged according to (51). Wild-type strains of *C. elegans* were variety Bristol, strain N2. Strains were maintained by standard methods (52). Integrated transgenes and transgenes maintained as extrachromosomal arrays included: *kyIs140 [str-2p::GFP, lin-15(+)] I* (31), *vyEx1089, 1090 [odr-3p::tba-9::SL2::TagRFP; ofm-1p::DsRed],* and *vyEx1091, 1092, 1093 [odr-3p::tba-9*$^{D256A/E259A}$*::SL2::TagRFP; ofm-1p::DsRed].*

Microinjection

Capped, synthetic mRNAs were dissolved in water and injected into embryos in 3% Ficoll using standard methods (18). mRNA injections were made using borosilicate glass needles calibrated to bubble pressures of 50-70 kPa in water, delivering 100 ms pulses. To avoid bias, injections were made directly into the animal pole. After 30 min, embryos were washed in 0.75X MMR for 30 min and cultured in 0.1X MMR until desired stages.

Laterality assays

Xenopus embryos were analyzed for position (situs) of three organs; the heart, stomach and gallbladder (53). Heterotaxic embryos were defined as having a reversal in one or more organs. Only embryos with normal dorsoanterior development and clear left- or right-sided organs were scored. Percent heterotaxia was calculated as the number of heterotaxic divided by the number of total scorable embryos (error bars indicate variability from eggs of individual females). A χ^2 test (with Pearson correction for increased stringency) was used to compare absolute counts of heterotaxic embryos.

***In Situ* hybridization**

Whole mount *in situ* hybridization was performed using standard protocol (54). *In situ* hybridization probes against Xnr-1 (the Xenopus nodal) mRNAs (22) were generated *in vitro* from linearized template using DIG labeling mix (Roche). Embryos injected with mutated tubulins were examined for Xnr-1 localization. A χ^2 test was used to compare absolute counts of embryos with correct versus incorrect Xnr-1 expression.

Quantitative Proteomics

Snap-frozen Xenopus embryos (n=30-50) in MeOH whose color and morphology at 4-cell stage clearly indicated the dorso-ventral axis were divided in half along the first cleavage plane. L and R sides were pooled and placed in a 20µl/embryo lysis buffer (see Supplemental Materials for details of protein digestion and buffer conditions). The resulting digested peptides were cleaned and desalted with C18

stage tips for direct LC-MS/MS analysis. nanoUPLC-MS/MS; Protein identification and Label Free Quantitation: to test the protein extraction protocol, the L and R sides of 50 pooled control embryos were first subjected to a pilot protein ID analysis via ultrahigh pressure liquid chromatography-mass spectrometry using Waters nanoACQUITY with AB Sciex 5600 Triple Tof mass spectrometer. To ascertain the quantitative protein differences between the two halves, the L and R pooled samples from 30 embryos were then subjected to Label Free Quantitation (LFQ) on a Thermo Fischer Scientific LTQ Orbitrap XL mass spectrometer containing the same Waters nAcquity system. All of the L and R side samples were randomized and 0.2µg of each of the enzymatically digested peptides was injected in 3 technical replicates with blank injected runs in between to minimize carry over. For the LFQ experiments, the LTQ Orbitrap is equipped with a Waters nanoAcquity UPLC system. The mass spectrometer acquired one survey run in the Orbitrap mode at 60,000 resolving power (400-2000 m/z) and 3 consecutive data dependent MS/MS runs in LTQ operating in CID mode. The raw data files were searched against a Xenopus database using Mascot search algorithm. In LFQ experiments the Mascot database search is integrated into the Non Linear Progenesis Software (www.nonlinear.com), which performs feature extraction (peptide m/z peaks), chromatographic and spectral alignment, data filtering, and statistical analysis. Proteins showing a significant ($p<0.05$, ANOVA and more than 3-fold difference in either direction) left- or right-sided bias in control embryos were selected as significant.

Human Cell Culture, Transfection and Microscopic Analysis

Culture of dHL60 cells and transfections were performed as described previously (Xu et al., 2003). For transient transfection, cells (on day 6 after addition of DMSO) were washed once in RPMI medium 1640-Hepes and resuspended in the same medium to a final concentration of 10^8 ml^{-1}. DNA was then added to the cells (50 µg of GFP-arrestin-3 plasmid), and the cell-DNA mixture was incubated for 10 min at room temperature, transferred to electroporation cuvettes, and subjected to an electroporation

pulse on ice at 310 V and low resistance. Transfected cells were allowed to recover for 10 min at room temperature and then transferred to 20 ml complete medium. Subsequent migration assays were performed 4 h after transfection. Live cells were allowed to stick to fibronectin-covered coverslips, and subjected to stimulation with a uniform concentration of fMLP (100 nM), and were imaged as previously described (55).

ACKNOWLEDGMENTS

We thank Claire Stevenson for assistance with molecular biology, Punita Koustubhan and Amber Currier for *Xenopus* husbandry, Erol Gulcicek, Christopher Colangelo, and Thomas Abbott for assistance with interpretation of proteomic data, and Laura Vandenberg and the other members of the Levin lab for useful discussions. ML gratefully acknowledges funding support from the NIH (R01-GM077425) and the American Heart Association (Established Investigator Grant 0740088N). Y.-W.H. was supported by a NIH Training Grant of Organogenesis; C.-F.C was supported by a Whitehall Foundation Research Award and an Alfred P. Sloan Research Fellowship.

REFERENCES

1. Peeters H & Devriendt K (2006) Human laterality disorders. (Translated from eng) *Eur J Med Genet* 49(5):349-362 (in eng).
2. Tabin C (2005) Do we know anything about how left-right asymmetry is first established in the vertebrate embryo? (Translated from eng) *J Mol Histol* 36(5):317-323 (in eng).
3. Vandenberg LN & Levin M (2009) Perspectives and open problems in the early phases of left-right patterning. (Translated from eng) *Semin Cell Dev Biol* 20(4):456-463 (in eng).
4. Aw S & Levin M (2009) Is left-right asymmetry a form of planar cell polarity? (Translated from eng) *Development* 136(3):355-366 (in eng).
5. Basu B & Bruedner M (2008) Cilia: multifunctional organelles at the center of vertebrate left-right asymmetry. *Ciliary Function in Mammalian Development,* Current Topics in Developmental Biology, ed Yoder BK (Elsevier Academic Press Inc, San Diego), Vol 85, pp 151-174.
6. Speder P, Petzoldt A, Suzanne M, & Noselli S (2007) Strategies to establish left/right asymmetry in vertebrates and invertebrates. (Translated from eng) *Curr Opin Genet Dev* 17(4):351-358 (in eng).
7. Gros J, Feistel K, Viebahn C, Blum M, & Tabin CJ (2009) Cell movements at Hensen's node establish left/right asymmetric gene expression in the chick. (Translated from eng) *Science* 324(5929):941-944 (in eng).
8. Armakolas A & Klar AJ (2007) Left-right dynein motor implicated in selective chromatid segregation in mouse cells. *Science* 315(5808):100-101.
9. Klar AJ (2008) Support for the selective chromatid segregation hypothesis advanced for the mechanism of left-right body axis development in mice. (Translated from eng) *Breast Dis* 29:47-56 (in eng).
10. Zhang Y & Levin M (2009) Left-right asymmetry in the chick embryo requires core planar cell polarity protein Vangl2. (Translated from Eng) *Genesis* 47(11):719-728 (in Eng).
11. Levin M & Palmer AR (2007) Left-right patterning from the inside out: widespread evidence for intracellular control. (Translated from eng) *Bioessays* 29(3):271-287 (in eng).

12. Vandenberg LN & Levin M (2010) Far from solved: A perspective on what we know about early mechanisms of left-right asymmetry. (Translated from eng) *Dev Dyn* 239(12):3131-3146 (in eng).
13. Abe T, Thitamadee S, & Hashimoto T (2004) Microtubule defects and cell morphogenesis in the lefty1lefty2 tubulin mutant of Arabidopsis thaliana. (Translated from eng) *Plant Cell Physiol* 45(2):211-220 (in eng).
14. Thitamadee S, Tuchihara K, & Hashimoto T (2002) Microtubule basis for left-handed helical growth in *Arabidopsis*. *Nature* 417(6885):193-196.
15. Nakamura M & Hashimoto T (2009) A mutation in the Arabidopsis gamma-tubulin-containing complex causes helical growth and abnormal microtubule branching. (Translated from eng) *J Cell Sci* 122(Pt 13):2208-2217 (in eng).
16. Abe T, Thitamadee S, & Hashimoto T (2004) Microtubule defects and cell morphogenesis in the lefty1lefty2 tubulin mutant of *Arabidopsis thaliana*. *Plant Cell Physiol* 45(2):211-220.
17. Ishida T, Kaneko Y, Iwano M, & Hashimoto T (2007) Helical microtubule arrays in a collection of twisting tubulin mutants of Arabidopsis thaliana. (Translated from eng) *Proceedings of the National Academy of Sciences of the United States of America* 104(20):8544-8549 (in eng).
18. Sive H, Grainger RM., Harland RM. (2000) *Early Development of Xenopus Laevis: A Laboratory Manual* (Cold Spring Harbor Laboratory Press, New York).
19. Vick P*, et al.* (2009) Flow on the right side of the gastrocoel roof plate is dispensable for symmetry breakage in the frog Xenopus laevis. (Translated from Eng) *Dev Biol* (in Eng).
20. Blum M*, et al.* (2009) Xenopus, an ideal model system to study vertebrate left-right asymmetry. (Translated from eng) *Dev Dyn* 238(6):1215-1225 (in eng).
21. Toyoizumi R, Ogasawara T, Takeuchi S, & Mogi K (2005) Xenopus nodal related-1 is indispensable only for left-right axis determination. (Translated from English) *Int. J. Dev. Biol.* 49(8):923-938 (in English).
22. Sampath K, Cheng AMS, Frisch A, & Wright CVE (1997) Functional differences among Xenopus nodal-related genes in left-right axis determination. (Translated from English) *Development (Cambridge, England)* 124(17):3293-3302 (in English).
23. Levin M (2003) Motor protein control of ion flux is an early step in embryonic left-right asymmetry. *Bioessays* 25(10):1002-1010.
24. Aw S, Adams DS, Qiu D, & Levin M (2008) H,K-ATPase protein localization and Kir4.1 function reveal concordance of three axes during early determination of left-right asymmetry. (Translated from Eng) *Mech Dev* 125:353-372 (in Eng).
25. Qiu D*, et al.* (2005) Localization and loss-of-function implicates ciliary proteins in early, cytoplasmic roles in left-right asymmetry. *Dev Dyn* 234(1):176-189.
26. Adams DS*, et al.* (2006) Early, H+-V-ATPase-dependent proton flux is necessary for consistent left-right patterning of non-mammalian vertebrates. *Development* 133:1657-1671.
27. Levin M, Thorlin T, Robinson KR, Nogi T, & Mercola M (2002) Asymmetries in H+/K+-ATPase and cell membrane potentials comprise a very early step in left-right patterning. *Cell* 111(1):77-89.
28. Bernstein BW & Bamburg JR (2010) ADF/Cofilin: a functional node in cell biology. (Translated from English) *Trends Cell Biol* 20(4):187-195 (in English).
29. Gu J*, et al.* (2010) ADF/cofilin-mediated actin dynamics regulate AMPA receptor trafficking during synaptic plasticity. (Translated from eng) *Nat Neurosci* 13(10):1208-1215 (in eng).
30. Roberts RM, Katayama M, Magnuson SR, Falduto MT, & Torres KE (2011) Transcript profiling of individual twin blastomeres derived by splitting two-cell stage murine embryos. (Translated from eng) *Biol Reprod* 84(3):487-494 (in eng).
31. Troemel ER, Sagasti A, & Bargmann CI (1999) Lateral signaling mediated by axon contact and calcium entry regulates asymmetric odorant receptor expression in C. elegans. *Cell* 99(4):387-398.

32. Chang C, Hsieh YW, Lesch BJ, Bargmann CI, & Chuang CF (2011) Microtubule-based localization of a synaptic calcium-signaling complex is required for left-right neuronal asymmetry in C. elegans. (Translated from eng) *Development* 138(16):3509-3518 (in eng).
33. Wan LQ*, et al.* (2011) Micropatterned mammalian cells exhibit phenotype-specific left-right asymmetry. (Translated from eng) *Proc Natl Acad Sci U S A* 108(30):12295-12300 (in eng).
34. Xu J*, et al.* (2007) Polarity reveals intrinsic cell chirality. (Translated from eng) *Proc Natl Acad Sci U S A* 104(22):9296-9300 (in eng).
35. Manner J (2001) Does an equivalent of the "ventral node" exist in chick embryos? A scanning electron microscopic study. *Anat Embryol (Berl)* 203(6):481-490.
36. Tian T, Zhao L, Zhang M, Zhao X, & Meng A (2009) Both foxj1a and foxj1b are implicated in left-right asymmetric development in zebrafish embryos. (Translated from eng) *Biochem Biophys Res Commun* 380(3):537-542 (in eng).
37. Serluca FC*, et al.* (2009) Mutations in zebrafish leucine-rich repeat-containing six-like affect cilia motility and result in pronephric cysts, but have variable effects on left-right patterning. (Translated from eng) *Development* 136(10):1621-1631 (in eng).
38. Zhao C & Malicki J (2007) Genetic defects of pronephric cilia in zebrafish. (Translated from eng) *Mech Dev* 124(7-8):605-616 (in eng).
39. Zeng H, Hoover AN, & Liu A (2010) PCP effector gene Inturned is an important regulator of cilia formation and embryonic development in mammals. (Translated from eng) *Dev Biol* 339(2):418-428 (in eng).
40. Gardner RL (2010) Normal bias in the direction of fetal rotation depends on blastomere composition during early cleavage in the mouse. (Translated from eng) *PLoS One* 5(3):e9610 (in eng).
41. Deinum EE, Tindemans SH, & Mulder BM (2011) Taking directions: the role of microtubule-bound nucleation in the self-organization of the plant cortical array. (Translated from eng) *Physical biology* 8(5):056002 (in eng).
42. Brown NA & Wolpert L (1990) The development of handedness in left/right asymmetry. (Translated from eng) *Development* 109(1):1-9 (in eng).
43. Kuroda R, Endo B, Abe M, & Shimizu M (2009) Chiral blastomere arrangement dictates zygotic left-right asymmetry pathway in snails. (Translated from Eng) *Nature* 462(7274):790-794 (in Eng).
44. Carneiro K*, et al.* (2011) Histone Deacetylase activity is necessary for left-right patterning during vertebrate development. (Translated from Eng) *BMC Dev Biol* 11(1):29 (in Eng).
45. Danilchik MV, Brown EE, & Riegert K (2006) Intrinsic chiral properties of the Xenopus egg cortex: an early indicator of left-right asymmetry? *Development* 133(22):4517-4526.
46. Yost HJ (1991) Development of the left-right axis in amphibians. (Translated from eng) *Ciba Found Symp* 162:165-176; discussion 176-181 (in eng).
47. Klar AJ (1994) A model for specification of the left-right axis in vertebrates. *Trends Genet* 10(11):392-396.
48. Levin M & Nascone N (1997) Two molecular models of initial left-right asymmetry generation. (Translated from eng) *Med Hypotheses* 49(5):429-435 (in eng).
49. Oviedo NJ & Levin M (2007) Gap junctions provide new links in left-right patterning. (Translated from eng) *Cell* 129(4):645-647 (in eng).
50. Mello C & Fire A (1995) DNA transformation. *Methods Cell Biol* 48:451-482.
51. Nieuwkoop PD & Faber J (1967) *Normal table of Xenopus laevis (Daudin).* ((North Holland Publ. Co.), Amsterdam) (English) p pp. vi + 243.
52. Brenner S (1974) The genetics of Caenorhabditis elegans. *Genetics* 77(1):71-94.

53. Levin M & Mercola M (1998) Gap junctions are involved in the early generation of left-right asymmetry. (Translated from eng) *Dev Biol* 203(1):90-105 (in eng).
54. Harland RM (1991) In situ hybridization: an improved whole-mount method for *Xenopus* embryos. (Translated from English) *Methods Cell Biol.* 36:685-695 (in English).
55. Xu J*, et al.* (2003) Divergent signals and cytoskeletal assemblies regulate self-organizing polarity in neutrophils. *Cell* 114:201-214.
56. Abe T & Hashimoto T (2005) Altered microtubule dynamics by expression of modified alpha-tubulin protein causes right-handed helical growth in transgenic Arabidopsis plants. (Translated from eng) *Plant J* 43(2):191-204 (in eng).

FIGURE LEGENDS

Figure 1. Tubulin mutations affect LR asymmetry prior to the first cleavage event. (A-C) Organ situs of st. 45 embryos scored by observation. (A) A wild-type embryo, ventral view, showing the normal arrangement of the stomach (yellow arrowhead), heart apex (red arrowhead) and gall bladder (green arrowhead). (B) A heterotaxic embryo (ventral view) showing reversal of all three organs, i.e. situs inversus, induced by misexpression of the tubulin mutant. (C) A heterotaxic embryo (ventral view) showing reversal of the heart. (D) Statistical comparison of heterotaxia levels scored at st. 45 in embryos injected with mutated α-tubulin mRNA at various early cleavage stages. (E) Breakdown of types of heterotaxia observed from embryos injected with mutated α-tubulin mRNA at the 1 cell stage. (F) Statistical comparison of heterotaxia levels in embryos injected with mutated Tubgcp2 mRNA at various early cleavage stages. (G) Breakdown of types of heterotaxia observed from embryos injected with mutated Tubgcp2 mRNA at the 1 cell stage. ** $p<<0.01$, Welch's t- test, sample sizes as noted in Table S1.

Figure 2. Tubulin mutations perturb sidedness of asymmetric gene expression in *Xenopus*. Embryos injected with either tub4a mutant or Tubgcp2 mutant were processed for in situ hybridization at stage 22 with an Xnr-1 probe. (A) Both tubulin mutants deviated significantly (denoted with double asterisks) from control embryos (Tub4a: 64.7% incorrect expression, n = 51, $p<<0.01$ Welch's t-test; Tubgcp2: 32.5 % incorrect expression, n = 83; control: 7.33% incorrect expression, n=150, $p<<0.01$ Welch's t-test). (B-D) Xnr-1 expression pattern (purple stain) characterized in tubulin mutant mRNA-injected embryos; (B) left expression indicated by one red arrow and one white arrow, (C) absence of expression as indicated by two white arrows, (D) bilateral expression as indicated by two red arrows.

Figure 3. Tubulin mutations alter biased Cofilin-1 expression. (A) tdTomato:Cofilin-1a fusion mRNA was injected into *Xenopus* embryos either alongside tub4a mutant mRNA, tubgcp2 mutant mRNA or on its

own. (B) Injections were made shortly after fertilization; embryos were reared to stage 45 before scoring for tdTomato fluorescent signal. (C) Control embryos, injected with solely the tdTomato fluorescent marker displayed virtually no bias for signal localization (L localized : Right localized ratio = 0.89, N=117), whereas tdTomato:Cofilin-1a injected embryos displayed a leftward bias (L:R ratio = 1.50, N=103). Embryos that had been co-injected with the tdTomato:Cofilin-1a and a tubulin mutant (either tub4a or tubgcp2) resulted in reversals in this bias (0.63 L:R ratio in tub4a mutant, N=40; L:R ratio = 0.56 in tubscp2 mutant, N=98). (D) tdTomato expression patterns observed in stage 45 *Xenopus* embryos. * $p<0.05$; ** $p<0.01$.

Figure 4. Mutant tubulin disrupts LR asymmetry in *C. elegans* embryos and cultured dHL60 cells. (A) Wild-type *C. elegans* generate one AWC^{ON} olfactory neuron cell, which expresses the reporter gene *str-2p::GFP*, and one AWC^{OFF} cell, which does not (31). (B) *C. elegans* bearing mutations in aspartic acid (256th) and glutamic acid (259th) residues in α-tubulin exhibit a 2 AWC^{ON} phenotype at a frequency significantly higher than that caused by expression of wild-type TBA-9. These frequencies are quantified in (C). Differentiated HL-60 cells were transiently co-transfected with GFP-Arrestin-3 (as marker of MTOC) and wild type tub-a6 (D) or mutant tub-a6 (E), and then exposed to uniform fMLP (100 nM), which induced polarization. The red arrow is drawn through the center of the nucleus, pointing to the centrosome, at 0 sec as described previously (34). Final centrosome positions are indicated by the blue dots, relative to all red arrows co-aligned. While wild type tub-a6 does not affect the leftward bias, mutant tub-a6 abolishes it (χ^2 test, $p<0.01$). Bar, 20 μm.

Supplemental data captions

Figure S1. α-Tubulin and the γ-tubulin associated protein complex, Tubgcp2, are highly conserved among organisms. (A) Amino acid sequence alignment of the alpha/beta domain interface in various alpha tubulin orthologs. The conserved Ala180 (indicated with an arrowhead) was substituted with Phe in *Xenopus laevis* α-Tubulin mutants, as in the *lefty2 Arabidopsis* mutants. (B) Amino acid sequence alignment of the Grip motif 1 in various GCP2 orthologs (known as Tubgcp2 in *Xenopus*). The conserved Gly453 was substituted with Arg in Tubgcp2 mutants, as in *spr3 Arabidopsis* mutants.

Figure S2. Early injections give rise to functional proteins by the first cleavage. (A) Injections of mRNA encoding tdTomato:cofilin fluorescent protein fusions were performed shortly after fertilization into one side of the egg (off-center). Embryos were allowed to develop to the late 2-cell stage. (B) Embryos were processed for immunohistochemistry with an anti-RFP antibody showing expression of cofilin protein is already strong by the 2-cell stage, consistent with our ability to exert functional changes at the 2-cell by injections made soon after fertilization..

Figure S3. Heterotaxia rates in tdTomato:Cofilin-a1 co-injections. Embryos injected with cofilin constructs were scored for positioning of the heart, gut, and gall-bladder at st. 45. All of the cofilin constructs, but not the controls (injected with the fluorescent protein tdTomato alone) exhibited low but significant levels of heterotaxia. N's are given in the figure; Student's T test was used for significance calculations; * denotes $P<0.05$, ** denotes $P<0.01$.

Figure S4. Injection into one of two early blastomeres allows targeting of the L or R side of embryo. Embryos were injected in one blastomere of the 2-cell frog embryo with mRNA encoding the enzyme β-galactosidase. At st. 45, the embryos were developed using a chromogenic reaction, illustrating that mRNA injected in this manner targets cells on one side of the embryo – the first cleavage plane is indeed usually aligned with the prospective left-right midline of the embryo; as in numerous studies, where one

blastomere injection at the 2-cell stage allows the other side to serve as an unaffected contralateral control, this confirms our ability to target early injections of cofilin to one side or the other.

Figure S5. A model for tubulin's role in LR asymmetry in *Xenopus* embryos. (**A**) In unperturbed embryos, the right-biased cytoskeleton (24, 25) is likely to derive from the orientation of the microtubule organizing center (centriole) with respect to the dorso-ventral and animal-vegetal axis, as proposed originally for a chiral "F-molecule" (42). Correct function of both α-tubulin (determining the structure of the microtubules along the animal-vegetal axis, and those involved in the dorso-ventral axis induction at cortical rotation shortly after fertilization) and γ-tubulin (mediating anchoring of LR-oriented microtubules to the MTOC) results in the proper linkage of the MTOC to the two axes, allowing intracellular transport of LR determinant cargo molecules (11) to the right side which ultimately results in correct organ *situs*. (**B**) Mutations in the GTPase-activating domain of tubulin suppress correct microtubule dynamics and promote polymerization(56). Thus, the previously described (24) subtle right-ventral bending of the cytoskeleton would be altered when mutated α-tubulin and γ-tubulin subunits were introduced at the early 1-cell stage. In the absence of rightward intracellular transport of maternal proteins important for subsequent LR patterning steps, the downstream steps are randomized, resulting in a mixture of wild-type and heterotaxic embryos.

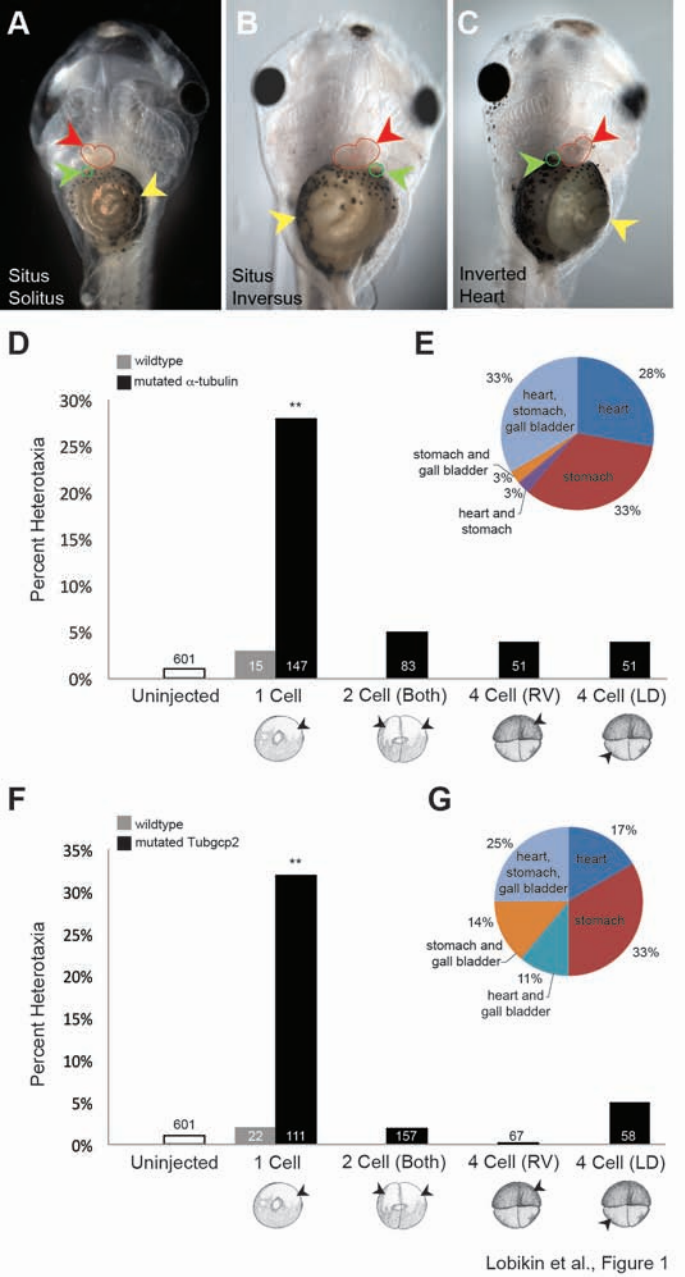

Lobikin et al., Figure 1

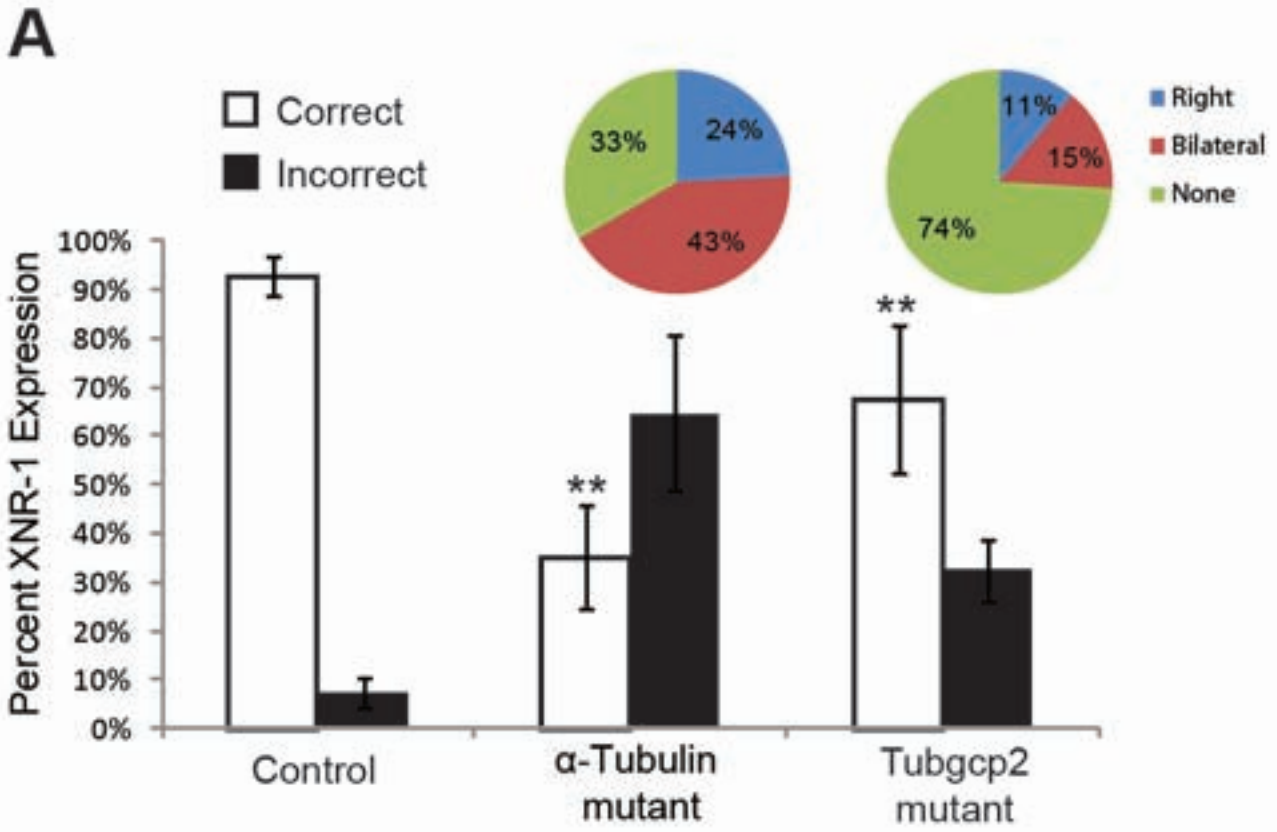

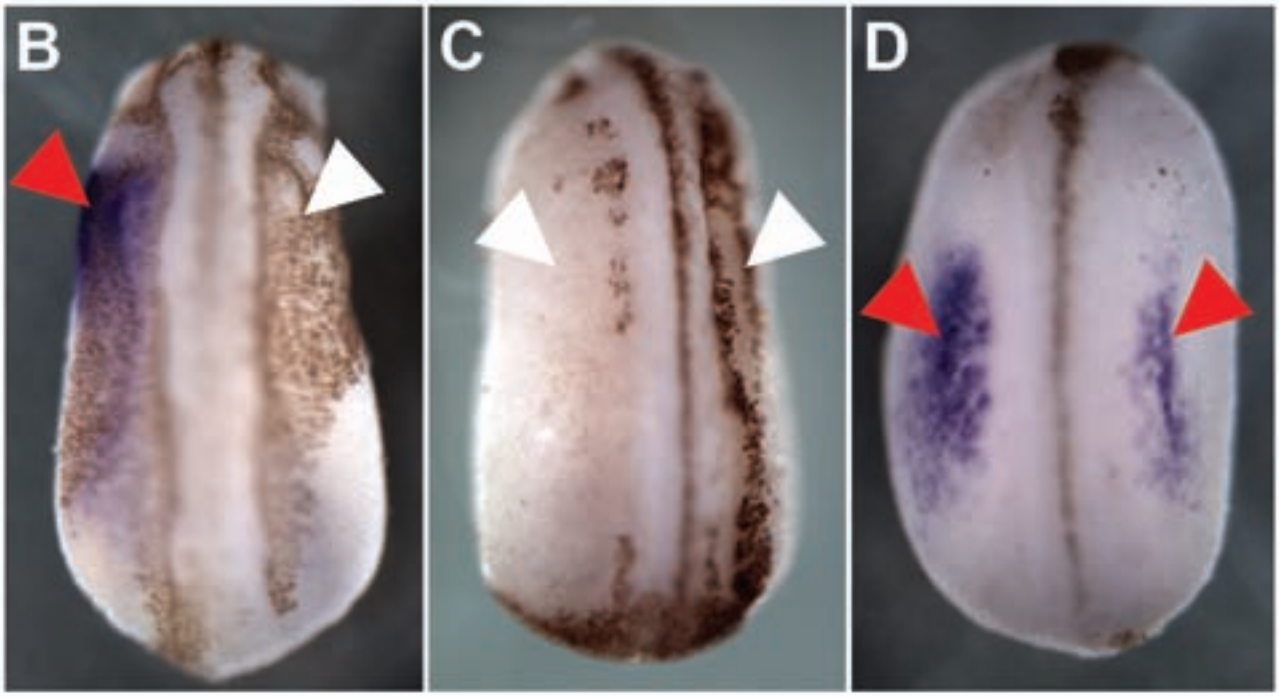

Lobikin et al., Figure 2

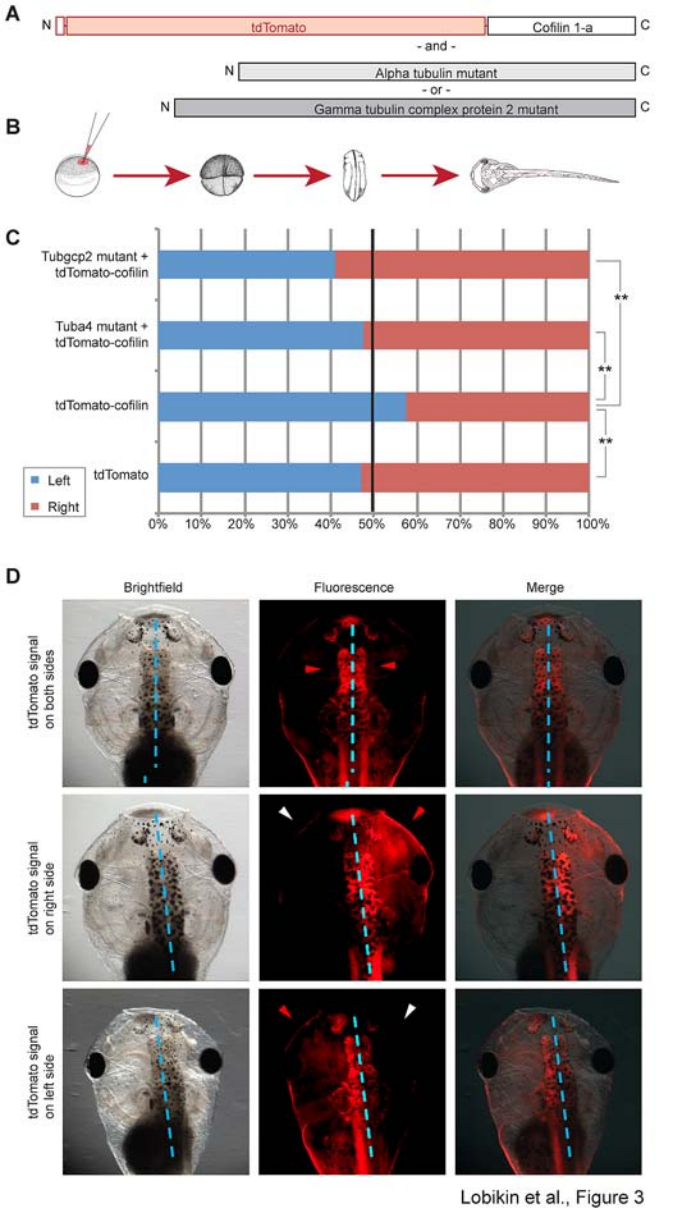

Lobikin et al., Figure 3

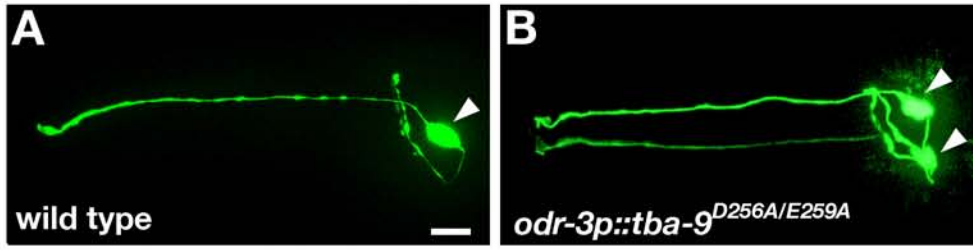

C

Genetic Background	2AWC^{OFF} (%)	1AWC^{OFF}/1AWC^{ON} (%)	2AWC^{ON} (%)	n
Wild type	0	100	0	77
odr-3p::tba-9	13	82	5	366
odr-3p::tba-9$^{D256A/E259A}$	13	42	45*	108

*$p < 0.0001$ compared to *odr-3p::tba-9*

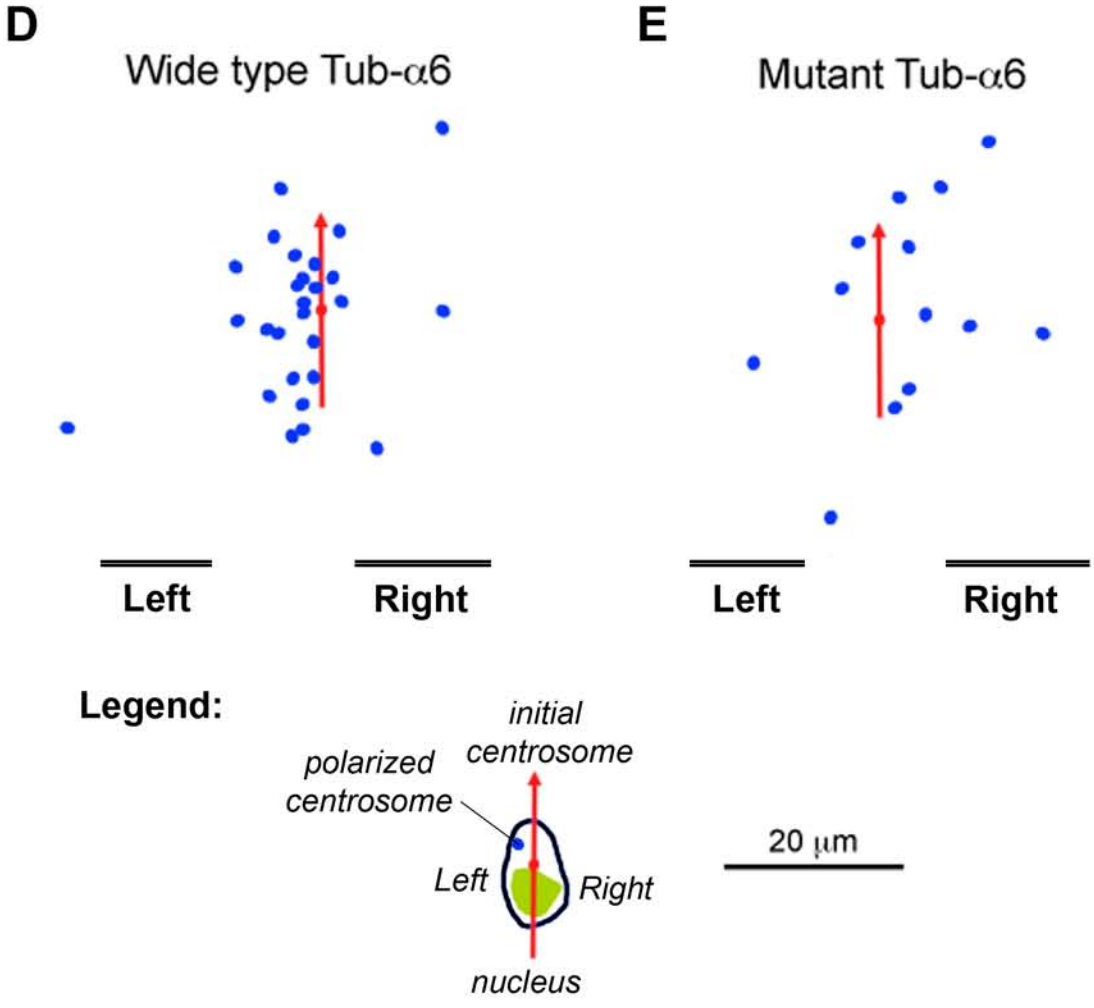

Table 1. **Protein localization bias is abolished by tubulin mutants for certain proteins**. Ratios were calculated for the relative abundances of each protein in the Left vs. Right halves of the embryo (using only those with Anova p-values <0.05). Proteins whose bias in control embryos was eradicated with the introduction of tubulin mutations are included below. P-values calculated between control ratios and those resulting from mutant tubulin injections.

Protein	Bias in Control Embryos Ratio (L:R)	Bias in αTubulin mutant embryos Ratio (L:R)	Significance	Bias in Tubgcp2 mutant embryos Ratio (L:R)	Significance
Interferon-related developmental regulator 2	5.6	**1.2**	**	**0.78**	**
Nucleolin (LOC397919 protein)	4.1	**1.1**	**	**0.95**	**
Nucleolin	2.9	**0.87**	***	**0.98**	***
Protein kinase C-binding protein NELL1	2.1	**0.92**	*	**0.80**	**
Rab-like protein 3	1.9	**1.1**	**	**0.85**	**
Thioredoxin domain containing protein	1.9	**1.1**	*	**1.0**	
Ribose-5-phosphate isomerase-like	1.9	**0.92**	*	**1.0**	*
DnaJ homolog subfamily C member 9-like	1.7	**1.2**	**	**0.89**	***
Cystatin-B	1.7	**1.3**	***	**1.0**	***
Eukaryotic initiation factor 4A-III-B	1.7	**0.82**	***	**1.0**	***
Dynactin subunit 2-A	1.6	**1.1**	*	**0.89**	**
Frizzled-1	1.6	**1.1**	*	**0.76**	*
Cofilin-1-B	1.5	**1.2**	*	**1.1**	**
Cofilin-1-A	1.4	**1.1**		**1.1**	
Ionotropic glutamate receptor	0.58	**0.88**	*	**1.3**	*
Nonmuscle myosin II heavy chain A	0.57	**1.3**	***	**1.1**	*
Nascent polypeptide-associated complex subunit alpha	0.53	**1.2**	*	**1.2**	**
Transcription factor BTF3 homolog 4	0.43	**1.0**	**	**0.90**	**
Electron transfer flavoprotein subunit beta-like	0.39	**1.1**	*	**0.73**	**
u6 snRNA-specific terminal uridylyltransferase 1	0.06	**1.7**	**	**0.76**	**
40S ribosomal protein S13 ±	0.05	**1.0**	*	**1.2**	*

*** P<0.001, ** P<0.01, * P<0.05